Phonon Mean Free Path in Silicon Between 77 and 250°K*

R. Gereth and K. Hubner†

Shockley Research Laboratory, Clevite Corporation, Palo Alto, California

(Received 28 October 1963)

Measurement of transmitted phonon drag across 10 ohm cm p-type silicon indicates a phonon mean free path of the relevant thermal phonons which varies from about 80 μ at 77°K to 12 μ at 250°K. The values depend on the method of evaluation. A simplified analysis suggests that below 150°K the longitudinal acoustic branch of the phonon spectrum is dominant.

I. INTRODUCTION

TRANSMITTED phonon drag[1-3] in diffused silicon npn structures is employed to measure the phonon mean free path in the temperature range between 77 and 250°K. The geometry of the test samples used is shown in Fig. 1. An applied electric field $\mathbf{E}_1$ in the top n layer of thickness L_1 sets up a drift velocity of the electrons. Momentum is transferred from the electrons to those phonons (called the relevant phonons) which can interact with them. The electron current thus produces a source of relevant phonons in the n layer. This disturbance from the thermal phonon equilibrium propagates through the p layer of thickness W_p and acts upon the electrons in the bottom n layer, thereby setting up an induced electric field $\mathbf{E}_2$ opposite in direction to $\mathbf{E}_1$. The ratio $|E_2/E_1|$ is a measure of the relevant phonon momentum reaching the bottom n layer. The strength of this disturbance of the phonon-equilibrium distribution will die away along the z direction with a characteristic mean free path L_ϕ. This is due to phonon-phonon scattering which will tend to restore thermal equilibrium, and also to phonon-defect scattering[3-5] such as interaction with impurity atoms, vacancy clusters, dislocations, and other defects. Measurement of $|E_2/E_1|$ for a set of samples differing only in the width W_p will therefore yield information on the mean free path L_ϕ of the relevant phonons. Repeating these measurements at different temperatures will in addition reveal the temperature dependence of the phonon mean free path. The present paper reports about those investigations putting main emphasis on the description of the experiments and measurements performed. This is followed by a qualitative discussion of the results.

In the Appendices an analysis based on a strongly simplifed theory is presented.

II. EXPERIMENT

A. Sample Preparation

The silicon single crystals used were pulled from the melt contained in a quartz crucible.[6] They were doped to yield a boron impurity concentration of 1.4×10^{15} cm^{-3}. The direction of growth was [100]. Slices of different thicknesses were cut perpendicular to the growth axis and diffused with phosphorus at 1300°C, resulting in a junction depth of 15 μ and a surface concentration of 1.2×10^{18} cm^{-3} for one group and 1.4×10^{18} cm^{-3} for another. The samples were then cut from these slices according to Fig. 1 and had the following typical dimensions: $X = 10$ mm; $Y = 1$ mm. The over-all thicknesses of the samples varied between 42 and 150 μ, depending on the width of the middle p layer. The (xy) surfaces were mechanically lapped to give diffuse phonon reflection, while the sides were chemically polished. Contacts were applied by thermal compression of 0.003-in.-diam gold wires.

B. Apparatus

The electrical arrangement to measure the transmitted phonon drag signal was essentially the same as that used in earlier experiments.[2] The primary current was supplied by a square-wave generator to the top n layer. Two additional pickup probes on the top layer (see Fig. 1) served to monitor the resulting input field. Two probes on the bottom n layer picked up the transmitted phonon-drag signal, which was amplified in a

[1] W. Shockley, in *Structure and Properties of Thin Films*, edited by C. A Neugebauer, J. B. Newkirk, and D. A. Vermilyea (John Wiley & Sons, Inc., New York, 1959), pp. 306–326.

[2] K. Hubner and W. Shockley, Phys. Rev. Letters 4, 504 (1960).

[3] K. Hubner and W. Shockley, *Proceedings of the International Conference on Semiconductor Physics, Prague, 1960* (Czechoslovakian Academy of Sciences, Prague, 1961), p. 299.

[4] K. Hubner and W. Shockley, Advan. Energy Conver. 1, 93 (1961).

[5] K. Hubner and W. Shockley, in *Proceedings of the International Conference of the Physics of Semiconductors, Exeter* (The Institute of Physics and Physical Society, London, 1962), p. 157.
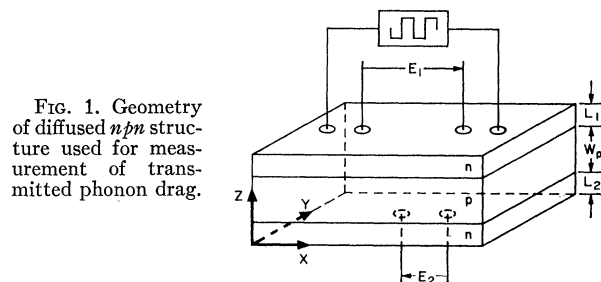

FIG. 1. Geometry of diffused npn structure used for measurement of transmitted phonon drag.

[6] J. Czochralski, Z. Physik. Chem. 92, 219 (1917).

Tektronics No. 122 amplifier and then displayed on a Tektronics 503 oscilloscope. The two pickup probes on the output side of the specimen were moved inward to avoid the effect of ordinary thermoelectric voltages due to power dissipation at the current-carrying input contacts. If a primary signal of sufficiently high frequency or fast rise time is used, any temperature gradient which may exist between the two pickup probes will not be able to follow the frequency of the applied signal, because the thermal time constant is too long. The square-wave signal used had a frequency of approximately 50 cps and a total rise time of less than 100 μsec.

The experimental setup for measuring the transmitted phonon drag as a function of temperature is illustrated in Fig. 2. It consists of an evacuated thin-walled stainless-steel enclosure containing a gold-plated copper block representing a high heat capacity. A separate vacuum-tight inlet permits the copper heat sink to be either cooled by liquid nitrogen or slowly heated by a special heater. The sample is mounted on a small gold-plated copper pedestal which in turn is pressed against the copper block by a spring. The electrical insulation of the sample is established by thin mica foils. By first cooling the copper block to liquid-nitrogen temperature and then letting it gradually warm up with a small heater, one can measure samples over the entire temperature range from 77°K to room temperature. Temperature was measured by two iron-constantan thermocouples, one touching the sample on the top, the other being inserted into the copper pedestal. The thermocouples were calibrated at the temperatures of liquid nitrogen, dry ice, and ice water. In addition, the sheet conductivity of the input layer was also used as a "thermometer." This was particularly useful when measurements were carried out at different current levels. Heating up of the sample at high current levels could then be corrected for by comparison with the sheet conductance at very low current levels where the heating could be neglected.

III. MEASUREMENTS

Figure 3 shows measurements of $|E_2/E_1|$ versus absolute temperature T for five typical samples having values of the middle p layer W_p between 12 and 120 μ. Measurements were taken over a primary current range with a ratio of approximately 1 to 10, 30 mA being the upper limit. Every point in Fig. 3 represents a measurement at a given input current. This is the reason for the large number of points shown. The fact that all the points for a specific sample obtained at different current levels form a fairly smooth curve suggests that no effect due to heating caused by power dissipation in the samples interfered with the measurements. Such ordinary thermoelectric effects would vary with the electrical power dissipated and hence with the square of the input current.
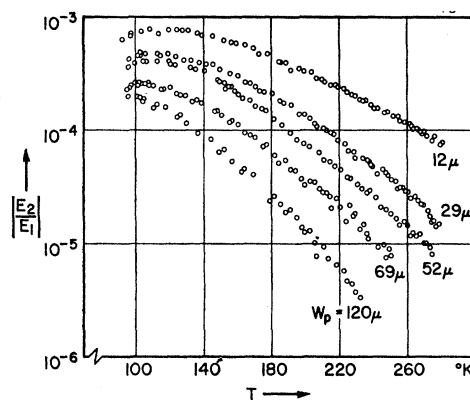

FIG. 3. Representative set of measurements of transmitted phonon drag versus temperature.
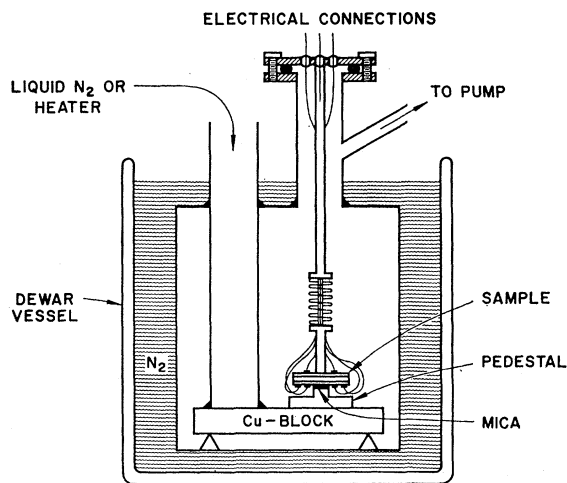
The measured $|E_2/E_1|$ values of the samples with $W_p = 12$ μ reach a clearly visible maximum at approximately 110°K. This extremum arises from the temperature dependence of the efficiency of transmitting and receiving n layers and is further discussed in the Appendix. In order to eliminate the temperature dependence of transmitter and receiver efficiency and to obtain information on the phonon mean free path within the p layer, the results have been redrawn and $|E_2/E_1|$ was plotted versus W_p with the temperature as a parameter. This is shown in Fig. 4. Several samples have been measured for each thickness W_p. The data on Fig. 4 represent the average values for all samples measured, not only those presented in Fig. 3. It is seen that the measured transmitted phonon-drag signals for $W_p = 69$ μ, and especially those for $W_p = 29$ μ, fall slightly below the curve smoothly connecting the values for $W_p = 12$, 52, and 120 μ. This result arose from the fact that the silicon slices used for the preparation of the samples with $W_p = 12$, 52, and 120 μ were predeposited with

FIG. 2. Arrangement employed to sweep the temperature range from 77 to 250°K.

phosphorus and diffused in one batch while those for the $W_p = 29$ and $69\ \mu$ samples were processed in another one. The latter had a slightly higher phosphorus concentration in the outer layers, as mentioned in "Sample Preparation," which subsequently reduced the efficiency of transmitting and receiving n layers.[3] The curves of Fig. 4 have been drawn to take this fact into account.

IV. DISCUSSION OF EXPERIMENTAL RESULTS

Because transmitter and receiver efficiency stays constant at a given temperature, one should be able to extract information on the phonon mean free path from the family of curves represented in Fig. 4. One simple method is to determine the slope for each curve and to calculate the mean free path from this value. As can be seen, however, the curves of Fig. 4 are not straight lines on semilogarithmic paper. This arises from the fact that the relevant phonons are not monochromatic and that different wavelength phonons have different mean free paths.[7] The intermediate p layer tends to filter
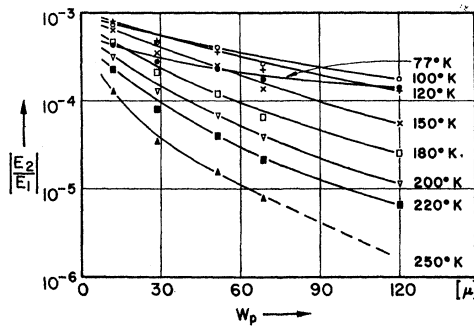

FIG. 4. Transmitted phonon drag versus thickness W_p of middle p layer.

the higher energy phonons which have shorter mean free paths so that the curves in Fig. 4 flatten out with increasing W_p. In order to avoid this filtering and to obtain an average mean free path L_ϕ of most of the phonons involved, L_ϕ should be determined from the slope at the smallest possible value of W_p. This was done by evaluating the curves of Fig. 4 at $W_p = 10\ \mu$. The results are plotted in Fig. 5. As can be seen from this graph the phonon mean free path in silicon due to phonon-phonon scattering is larger than $10\ \mu$ over the temperature range between 77 and 250°K; therefore, relatively little filtering should have taken place for the phonons penetrating a $10\ \mu$ wide p layer, especially at low temperatures.

Above a certain critical temperature one might have expected the onset of multiphonon processes to produce a distinct additional decrease of transmitted phonon-drag signal and correspondingly of phonon mean free path. The curves of Fig. 3, however, are smooth from 100 to 260°K and do not exhibit such a behavior, sug-
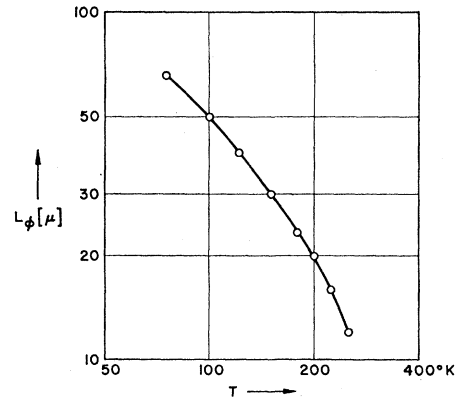
[7] C. Herring, Phys. Rev. 95, 954 (1954).

FIG. 5. Phonon mean free path L_ϕ as a function of temperature. L_ϕ is determined at $W_p = 10\ \mu$ from the slope of curves presented in Fig. 4.

gesting that this onset does not occur within the temperature range measured.

The direct determination of L_ϕ from the slope at a particular value of W_p does not take into account the angular dependence of the disturbed phonons on the direction of the applied field. Most phonons are incident on the p layer with an angle difference from $\frac{1}{2}\pi$ and therefore must travel further than W_p to reach the receiving layer. This, and also the filtering effect, make it desirable to employ an evaluation technique which uses the shape of the entire curve to determine a phonon mean free path. This is done in the Appendix, where normalized curves for $|E_2/E_1|$ versus W_p were calculated under very stringent and simplifying assumptions. Comparing the families of calculated curves with the experimental results permitted the determination of certain phonon mean free paths for every curve of Fig. 4. The data obtained in this way agree reasonably well with the ones plotted in Fig. 5. Furthermore, the analysis presented in the Appendix suggests the speculation that below 150°K the longitudinal acoustical branch of the phonon spectrum may be dominant, while at higher temperatures an admixture of transverse phonons seems likely.

ACKNOWLEDGMENTS

The authors are very grateful to Dr. C. Herring of Bell Telephone Laboratories for suggesting the study of the temperature dependence of the phonon mean free path and for several stimulating discussions. They also thank Dr. W. Shockley and Professor Dr. G. Busch for their interest in this work.

APPENDIX

A. Efficiency of the Phonon Transmitting and Receiving N Layers

Figure 5 shows that the phonon mean free path in the p region is larger than $12\ \mu$ over the temperature range measured. Therefore, one would not expect a great

influence of phonon scattering in the p layer upon the shape of the $W_p = 12\ \mu$ curve in Fig. 3, especially at the low end of the temperature range. Consequently, the maximum at 110°K must arise only from the temperature dependence of the efficiency of the phonon-transmitting and receiving n layers. This can be understood semiquantitatively using Herring's model[8] to describe phonon drag in terms of electron and phonon drift velocities. The same model has also been adopted by Shockley[1] to describe the transmitted phonon drag.

In Ref. 2 the ratio of the transmitted phonon drag signal E_2 to the input signal E_1 has been calculated for the symmetrical npn structure. To analyze only the behavior of the outer n layers one can simplify the above quoted expression for the case of a three-layer npn structure with negligible width W_p of the p layer. If one further assumes that the phonon mean free path in the n layers is always small compared to the depth of the n layers, then one obtains the following expression:

$$\left|\frac{E_2}{E_1}\right| \sim \frac{1}{(1+n/n_i)(1+n_\phi/n)(1+n/n_\phi)}. \quad (1)$$

Equation (1) describes the relative effectiveness of the outer n layers as phonon transmitter and receiver, in a symmetrical homogeneously doped sample, as a function of electron concentration n. The symbols n_ϕ and n_i denote reference-electron densities. The first bracket in the denominator of Eq. (1) takes into account the reduction of the electron-drift velocity due to ionized impurity scattering in the input layer. The electron density at which lattice and impurity scattering of electrons are equal is called n_i. Mobility measurements as a function of electron concentration[9] yield n_i.

The second term in Eq. (1) expresses how phonon-phonon scattering reduces the resulting phonon-drift velocity in the input layer, which otherwise would be equal to the electron-drift velocity. The specific electron density at which the relevant phonons interact with the same strength with other phonons as they do with electrons is called n_ϕ. This quantity can be determined from the saturation effect of the thermoelectric power.[10] Finally, the third term of Eq. (1) takes into account how the phonon drift velocity in the receiving layer is reduced by phonon-electron scattering. The densities n_ϕ and n_i were determined from the above cited references as a function of temperature. The results are shown in Table I. The n_ϕ values were obtained by finding the concentration at which the thermoelectric power of arsenic-doped-silicon samples is one-half of its maximum value. Subsequently, this room-temperature electron concentration had to be adjusted to the actual electron concentration at the particular temperature.

[8] C. Herring, in *Semiconductors and Phosphors*, edited by M. Schoen and H. Welker (Interscience Publishers Inc., New York, 1958), pp. 184–235.
[9] F. J. Morin and J. P. Maita, Phys. Rev. 96, 28 (1954).
[10] T. H. Geballe and G. W. Hull, Phys. Rev. 98, 940 (1955).

TABLE I. Reference densities n_ϕ and n_i used to calculate the efficiency of the n layers as a function of temperature.

$T[°K]$	$n_\phi[\text{cm}^{-3}]$	$n_i[\text{cm}^{-3}]$
60	1.2×10^{15}	1.3×10^{15}
80	8.0×10^{15}	8.0×10^{15}
100	2.7×10^{16}	1.6×10^{16}
150	2.3×10^{17}	4.0×10^{16}
200	1.2×10^{18}	7.0×10^{16}

The n_i's were found by determining the electron concentration which halved the lattice mobility of the same silicon samples and then reducing the room-temperature concentration to the actual concentration at the particular temperature.

The electron reference densities of Table I were inserted into Eq. (1) and the relative value of $|E_2/E_1|$ were calculated for three different electron concentrations at room temperature.[11] The result, adjusted for easy comparison with the experiment, is shown in Fig. 6, where the dashed line indicates measurements for the sample of Fig. 3 with $W_p = 12\ \mu$. The points represent the calculated values. It is seen that transmitter and receiver efficiency will indeed go through a maximum which decreases and shifts toward higher temperatures for higher electron concentrations. The experimental curve measured on samples with a surface electron concentration at room temperature of $n_s = 1.2 \times 10^{18}$ cm^{-3} and a concentration at the junction of $n_j = 1.4 \times 10^{15}$ cm^{-3} has its maximum at a slightly higher temperature than the indicated curve for a homogeneous n layer with $n_{RT} = 1.3 \times 10^{17}$ cm^{-3}. This latter figure appears to be a reasonable value for an effective average-electron concentration in the investigated samples. A more accurate analysis is complicated by the fact that the electron concentration in the n layer follows a Gaussian distribution due to the diffusion technique used to dope these regions. But even in its present simple form the analysis fully accounts for the observed maxima in Fig. 3.

Measurements on samples with a larger value of W_p cannot be compared with the curves of Fig. 6, as phonon-phonon scattering in the intermediate p layer will reduce the observable $|E_2/E_1|$ values.

B. Evaluation of Phonon Mean Free Path

An attempt was made to develop a technique suitable for determining the phonon mean free path using the entire shape of the set of curves presented in Fig. 4. The calculation outlined below is based on the following assumptions:

1. The relevant phonon distribution is given by a Debye type spectrum of the form k^{-1} (k being the wave number) with a cutoff at k_0, which represents the highest

[11] The data for the electron concentration were taken from the silicon samples No. 126, 129, and 139, respectively, of Ref. 10.

wave number phonon which can interact with electrons.

2. Either longitudinal or transverse phonons are present.

3. The phonon mean free path depends on k as k^{-1} for transverse and k^{-2} for longitudinal acoustical phonons.[7] (More recent studies[12] indicate deviations from these ideal small wave number phonon scattering laws.)

4. The electron distribution is spherical.

5. Phonon-phonon scattering is dominant.

The coordinate system chosen for this calculation is shown in Fig. 7. In the same figure it is also indicated how the electron distribution is offset by the applied electric field E_1. The crosshatched area represents the angular distribution of the relevant electron or phonon momentum. The phonon-drift momentum F reaching the output layer, which in turn is proportional to the observable field E_2, is of the following form

$$F \sim \int_{k=0}^{k_0} \int_{\theta=0}^{\pi/2} \int_{a=0}^{\pi/2} \left[(k \sin\theta \sin\alpha)(k^{-1})(\sin\theta \sin\alpha) \right.$$
$$\left. \times \exp\left(-\frac{W_p}{L_{\phi\phi}(k) \cos\theta}\right)(k^2 \sin\theta dk d\theta d\alpha) \right]. \quad (2)$$

The first term of the integral denotes the component of the phonon wave vector in the direction of E_1. The second term approximates the relevant phonon distribution. The third term describes the decrease of the drift component for directions other than that of E_1 and is equal to the cosine of the angle between E_1 and k (see Fig. 7). The fourth term is the exponential scattering factor which describes the phonon scattering in the intermediate p layer. In the exponent is the ratio of the two lengths $W_p/\cos\theta$ and the mean free path $L_{\phi\phi}$ which is a function of phonon wave number. The symbol $L_{\phi\phi}$ is used to denote that only phonon-phonon scattering is considered and other effects such as phonon-
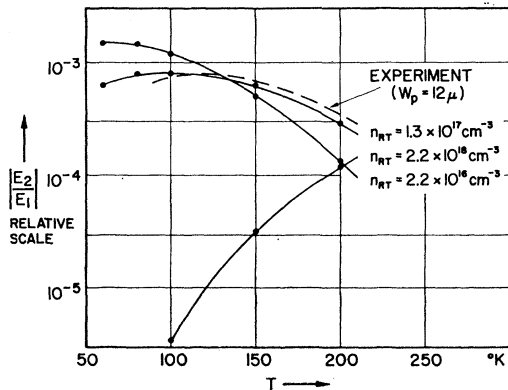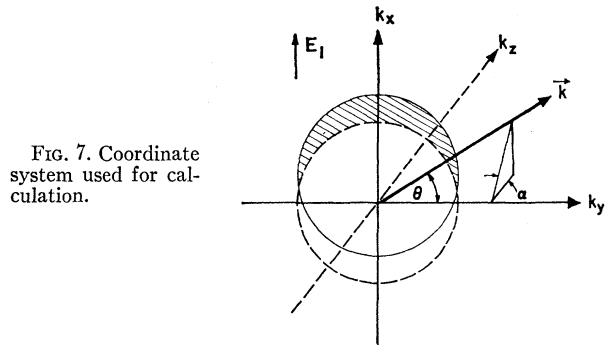

FIG. 7. Coordinate system used for calculation.

defect scattering or phonon-hole scattering are neglected. The last term is the volume element in k space. Since the shape of the experimental curves in Fig. 4 should be fitted, Eq. (2) was normalized by dividing this expression by the same term with W_p set equal to zero. This normalizes the phonon-drift momentum F_n reaching the output layer which will then be equal to 1 for $W_p = 0$.

The integration extends over the entire relevant phonon range up to the cutoff wave number k_0. The dependence of the phonon mean free path on the wave number has been assumed to be of the following form:

$$L_{\phi\phi}(k) = L_{\phi0}(k_0/k)^r, \quad (3)$$

where $L_{\phi0}$ is the mean free path of the highest energy relevant phonon with wave number k_0. The exponent r has been introduced as a parameter and will later be set equal to 2 for longitudinal and equal to 1 for transverse acoustical phonons, according to Herring.[7] By carrying out the elemental integrations in the normalized Eq. (2) and substituting the expressions

$$x = W_p/L_{\phi0}, \quad (4)$$

$$y^{-1} = (k_0/k)^r, \quad (5)$$

and

$$s = 3/r - 1, \quad (6)$$

one arrives at Eq. (7):

$$F_n = \tfrac{3}{2}(s+1) \int_0^1 \int_0^{\pi/2} \exp\left(-\frac{xy}{\cos\theta}\right) y^s \sin^3\theta dy d\theta. \quad (7)$$

The new variable y permitted elimination of k_0 from the result by transforming the upper limit of the integral over the wave number k to 1.

The integral (7) was graphically solved for

$r=2$, $s=\tfrac{1}{2}$ longitudinal branch, and

$r=1$, $s=2$ transverse branch.

The results which are a function of W_p and $L_{\phi0}$ only form two sets of curves (see Figs. 8 and 9) which can be fitted to the experimental data of Fig. 4 in order to determine $L_{\phi0}$ for $s=\tfrac{1}{2}$ or $s=2$, assuming that only one or the other branch is dominant.
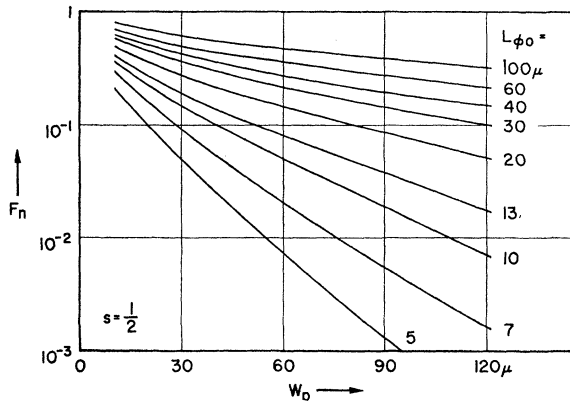

FIG. 6. Influence of electron concentration in input and output layer on $|E_2/E_1|$ as a function of temperature.

[12] C. Herring (private communication).

FIG. 8. Normalized transmitted phonon-drag curves for $s=\frac{1}{2}$ (longitudinal phonons).

The $L_{\phi 0}$ values obtained by this curve fitting are shown in Fig. 10, where also the mean free path determined from the slope at $W_p=10$ as given in Fig. 5 is indicated with points. As the experimental curves could not always be accurately fitted over the entire W_p range, the mean free paths obtained by fitting the range $W_p > 30$ μ were labeled with an A and with a B for the range $W_p < 30$ μ. The vertical widths of the cross-hatched stripes are therefore a measure of how well each experimental curve could be fitted with one of the calculated ones over the entire range of W_p at a certain temperature.
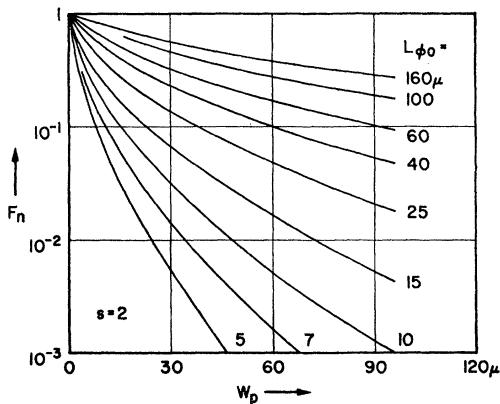

FIG. 9. Normalized transmitted phonon-drag curves for $s=2$ (traverse phonons).

C. Discussion of Results Summarized in Fig. 10

For the following one has to recall that the cross-hatched bands in Fig. 10 show the phonon mean free path $L_{\phi 0}$ of the highest wave number relevant phonon, assuming either only longitudinal ($s=\frac{1}{2}$) or only transverse ($s=2$) acoustical phonons. Because the mean free path of either branch decreases with increasing wave number [see Eq. (3)] one would expect the value determined from the slope at $W_p=10$ μ to be larger than that obtained from curve fitting. This should especially hold in the higher temperature range, where the mean free path becomes comparable with 10 μ and where part of the high-frequency relevant phonons have been filtered
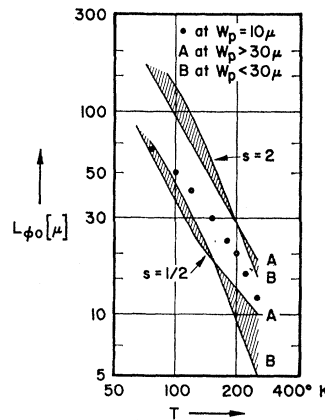

FIG. 10. Phonon mean free path $L_{\phi 0}$ versus temperature T as obtained from curve fitting and from slopes of curves in Fig. 4 at $W_p=10$ μ.

out by phonon-phonon scattering. Figure 10 exhibits this expected situation only for the $s=\frac{1}{2}$ case representing longitudinal phonons.

We therefore speculate that in the range between 77 and 150°K the longitudinal branch ($s=\frac{1}{2}$) may be dominant. This follows from the above mentioned fact that the solid circles fall about the $s=\frac{1}{2}$ curves as one would expect, while they fall way below those for $s=2$. The increasing difference between the circles and the $s=\frac{1}{2}$ curves is attributed to the filtering effect. Above 150°K there might be some admixture of transverse phonons. The basis for this is the poor fit which would be obtained for $s=\frac{1}{2}$, as indicated by the difference between curves A and B.